# Multinuclear MAS NMR Identification of Fluorine Species on the Surface of Fluorinated γ-Alumina

**ARTICLE** *in* THE JOURNAL OF PHYSICAL CHEMISTRY B · OCTOBER 2002

Impact Factor: 3.3 · DOI: 10.1021/jp0212489



**3 AUTHORS**, INCLUDING:

Roel Prins
ETH Zurich
**427** PUBLICATIONS **13,223** CITATIONS

# Multinuclear MAS NMR Identification of Fluorine Species on the Surface of Fluorinated $\gamma$-Alumina

**Weiping Zhang, Mingyong Sun,† and Roel Prins***

*Laboratory for Technical Chemistry, Swiss Federal Institute of Technology (ETH), CH-8093, Zurich, Switzerland*

*Received: May 21, 2002; In Final Form: September 5, 2002*

The fluorination on the $\gamma$-alumina surface was studied by multinuclear MAS NMR and BET measurements. The fluorine species on the fluorinated $\gamma$-alumina can be identified by $^{19}$F MAS NMR combined with $^{1}$H MAS NMR and $^{27}$Al MAS and CP/MAS NMR. As proven by $^{1}$H MAS NMR, fluorination of the alumina preferentially replaced the basic hydroxyl groups. Quantitative analysis showed that, at lower fluoride loadings, one alumina hydroxyl is substituted by one fluoride without breaking the bridging Al−O−Al bonds. At high fluoride content, more of the acidic hydroxyl groups are displaced by fluorine, and the number of added fluorine atoms exceeds the number of lost hydroxyl groups. Bridging Al−O−Al bonds are broken at high fluoride loading, and isolated $Al_xF_y{\cdot}nH_2O$ fractions appear as observed by $^{19}$F MAS and $^{27}$Al MAS NMR. Three types of fluorine species were detected in the $^{19}$F MAS NMR spectra of the fluorinated $\gamma$-alumina, which could be assigned to the fluorine species bound to one, two, and three octahedral aluminum atoms.

## Introduction

$\gamma$-$Al_2O_3$ is one of the most commonly used materials in the chemical and electronic industry. The hydroxyl groups on its surface play a crucial role in determining the properties of resultant alumina-based catalysts.[1] Fluorination of alumina by replacing hydroxyls has been shown to increase the rate of acid-catalyzed reactions such as cracking, isomerization, and polymerization.[2] In a supported catalyst such as Ni−Mo/$Al_2O_3$, the effects of fluorine on hydrodesulfurization and hydrodenitrogenation are thought to change the dispersion of the metal species in the oxidic precursor,[3] increase the sulfidability of the metal oxide,[4] increase the acidity,[5] and change the morphology of the metal sulfide surface.[6,7] The actual chemistry of the fluorine species and the causes of these effects are still not fully understood. Few studies have considered the structure of fluorine itself. This is partially due to the lack of a precise identification method for the fluorine sites on the surface of fluorinated alumina, although FT-IR has shown that fluorine can substitute for hydroxyl groups on its surface.[8] Poor resolution of the IR bands and possible differences in the extinction coefficients of different types of hydroxyl groups make it difficult, however, to quantitatively determine the distribution of the hydroxyl groups. $^{19}$F magic-angle spinning NMR (MAS NMR) is a direct and sensitive method for distinguishing different fluorine species in fluorinated amorphous alumina and aluminum oxophosphates.[9] However, it usually requires fast spinning rates to average the large homo- and hetero-nuclei dipolar interactions in solid samples that contain abundant nuclear spins such as $^{19}$F.[9] In our study, we applied an ultrafast spinning rate up to 29.5 kHz to reduce most of the $^{19}$F dipolar interactions and achieved high-resolution $^{19}$F MAS NMR spectra. $^{1}$H MAS NMR can provide quantitative information about variations in the hydroxyls if a proper compound is employed to calibrate the spectra of weighed samples, as shown previously.[10,11] A combination of $^{27}$Al MAS and cross-polarization MAS NMR, $^{19}$F MAS NMR, and quantitative analysis of $^{1}$H MAS NMR enable the identification of the fluorine species on the surface of fluorinated $\gamma$-alumina.

## Experimental Section

Fluorinated alumina ($Al_2O_3F$) with different F loadings was prepared by means of the incipient wetness impregnation method by impregnating $\gamma$-$Al_2O_3$ (Condea) with an aqueous solution of ammonium fluoride (Fluka) of appropriate concentration. The resultant fluoride contents were 0.5, 1.0, 3.8, and 10.8 wt % as calculated from the known amount of $NH_4F$ added. The samples were dried at 393 K for 4 h and calcined at 773 K for 4 h under air flow while slowly heating at a rate of 2 K/min in order to avoid evaporation of fluorine in the samples. This was checked semiquantitatively by X-ray fluorescence spectroscopy. Prior to the $^{1}$H → $^{27}$Al cross-polarization magic-angle spinning (CP/MAS) NMR experiments, the samples were hydrated completely in a desiccator with saturated $NH_4NO_3$.[12] Before acquisition of the $^{1}$H MAS NMR spectra, all of the samples were degassed at 673 K and a pressure below $10^{-2}$ Pa for 10 h.

Surface areas and pore volumes of all samples were measured at liquid-nitrogen temperature (77 K) on a Micromeritics TriStar-3000 instrument. Samples were outgassed at 673 K overnight before measurements. Surface areas were calculated using the BET model and a value of 0.162 nm$^2$ for the cross-sectional area of $N_2$. Pore volumes were estimated from t-plot calculations.

All of the NMR spectra were recorded on a Bruker AMX-400 spectrometer at room temperature. $^{27}$Al MAS NMR spectra with high-power proton decoupling were collected at 104.3 MHz using a 0.63 $\mu$s $\pi$/12 pulse with a 2 s recycle delay and 200 scans. $^{1}$H → $^{27}$Al CP/MAS spectra were recorded with a single contact, an optimized contact time of 0.9 ms, a recycle delay

* To whom correspondence should be addressed. Mailing address: Laboratory for Technical Chemistry. ETH−Hönggerberg, 8093 Zurich, Switzerland. Fax: +41−1−6321162. E-mail: prins@tech.chem.ethz.ch.
† Present address: Department of Chemical Engineering, University of Waterloo, Waterloo, Ontario N2L 3G1, Canada.

10.1021/jp0212489 CCC: $22.00 
Published on Web 10/23/2002

**TABLE 1: Surface Areas and Pore Volumes of $Al_2O_3F$ Samples**

| sample | surface area ($m^2/g$) | pore volume ($cm^3/g$) |
|---|---|---|
| $\gamma$-$Al_2O$ | 216 | 0.41 |
| 0.5% F/$Al_2O_3$ | 215 | 0.41 |
| 1.0% F/$Al_2O_3$ | 215 | 0.41 |
| 3.8% F/$Al_2O_3$ | 210 | 0.41 |
| 10.8% F/$Al_2O_3$ | 200 | 0.34 |

of 2 s, and 10 000−15 000 scans. The Hartmann−Hahn condition was established as described in the literature.[12,13] $^1$H MAS NMR spectra were measured at 400.2 MHz using single-pulse experiments with 2.2 $\mu$s $\pi/4$ pulse, a 4 s recycle delay, and 400 scans. A $\pi/4$ pulse with 4 s recycle delay was found sufficient for complete signal recovery. To obtain quantitative results, all of the samples were weighed, and the $^1$H MAS NMR spectra were calibrated by measuring a known amount of 1,1,1,3,3,3-hexafluoro-2-propanol (Fluka) under the same conditions.[10,11] Both $^{27}$Al and $^1$H MAS NMR spectra were recorded using 4-mm $ZrO_2$ rotors spun at 10 kHz, and chemical shifts were referenced to 1% aqueous $Al(H_2O)_6^{3+}$ and to tetramethylsilane, respectively. $^{19}$F MAS NMR experiments were performed at 376.5 MHz using 2.5-mm rotors at a spinning rate of 29.5 kHz, a recycle delay of 10 s, and 1600 scans. Spin−echo sequences ($\pi/2-\tau-\pi-\tau-$acquire) were used to reduce the fluorine background from the probehead, where $\tau$ was set to 508.47 $\mu$s (15 times the rotor period) to ensure no significant change of the line shape when compared with the single-pulse sequence, and the excitation pulse length was 1.5 $\mu$s ($\pi/2$). $^{19}$F chemical shifts were referenced to $CFCl_3$ at 0 ppm. For the quantitative determination of the fluorine species, all of the samples were weighed and measured under the same acquisition conditions. By varying the recycle delays in the $^1$H and $^{19}$F MAS NMR experiments, we found that the signal intensities had fully recovered after recycle delays of 4 and 10 s for the $^1$H and $^{19}$F spectra, respectively. Longer delay times did not increase the signal intensity. Therefore, these values were employed for the quantitative measurements in our study. The plots were drawn with the correction of the sample mass. The Dmfit program was employed for decomposition and integration of the spectra using proper Gaussian−Lorentzian line shapes.[14] The fitting errors for our spectra were estimated to be about 5%.

## Results

**Surface Area and Pore Volume.** The BET surface areas and pore volumes of $\gamma$-alumina with different fluoride loadings are listed in Table 1. It is clear that the surface area and pore volume hardly change with an increasing fluoride content up to 1.0 wt %. Further fluoride addition to 3.8 wt % leads to a slight decrease in the surface area. Significant decreases in the surface area and pore volume are observed when the fluoride content is increased to 10.8 wt %. This reveals that the structure of $\gamma$-alumina remains unchanged at lower fluoride loadings, whereas new material is formed at higher fluoride loadings, thus reducing the surface area and blocking the pores of the alumina support.

**$^{27}$Al MAS and $^1$H → $^{27}$Al CP/MAS NMR.** $^{27}$Al MAS NMR can provide information about the coordination numbers of the aluminum atoms in the $\gamma$-alumina. The application of $^1$H → $^{27}$Al cross-polarization technique can selectively enhance the Al signals of aluminum atoms which are coupled with protons of neighboring hydroxyls.[13] Figures 1 and 2 show the $^{27}$Al MAS and corresponding $^1$H → $^{27}$Al CP/MAS NMR spectra of $\gamma$-alumina with various fluoride contents. The alumina has two

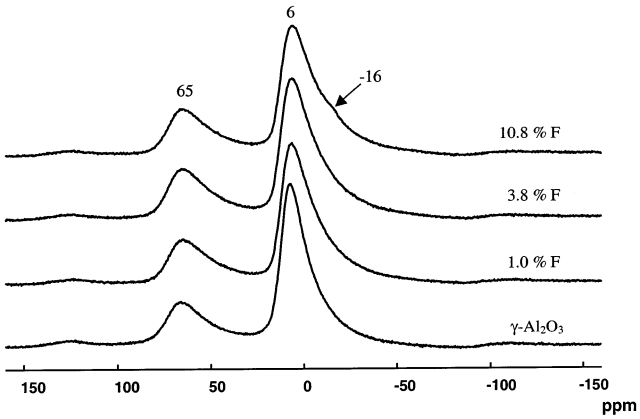


**Figure 1.** $^{27}$Al MAS NMR spectra of $\gamma$-$Al_2O_3$ with different fluoride loadings. The shoulder at −16 ppm is ascribed to six-coordinated aluminum in $Al_xF_y \cdot nH_2O$.

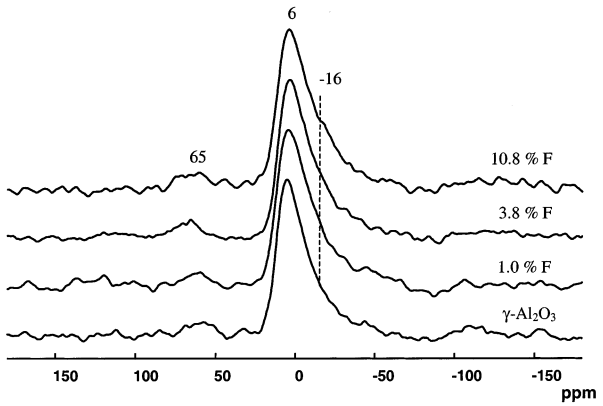


**Figure 2.** $^1$H → $^{27}$Al CP/MAS NMR spectra of $\gamma$-$Al_2O_3$ with various fluoride contents.

main signals. The signal at 65 ppm is attributed to four-coordinated aluminum, and the other at 6 ppm is ascribed to six-coordinated aluminum. Up to 3.8 wt % F, the peak intensities in the $^{27}$Al MAS NMR spectra are almost the same. With the further addition of fluoride to 10.8 wt %, the content of six-coordinated aluminum decreases and, at the same time, a shoulder centered at −16 ppm appears (Figure 1), which is assigned to six-coordinated Al in aluminum fluoride.[15] After $^1$H → $^{27}$Al cross polarization, the signal at 6 ppm increases greatly compared with that at 65 ppm. Thus, the hydroxyl groups in the alumina are mainly connected to six-coordinated aluminum. The peak at −16 ppm is also enhanced in the $^1$H → $^{27}$Al CP/MAS NMR spectrum of 10.8 wt % F/$Al_2O_3$. Thus, some of the six-coordinated Al in the alumina will be transformed to aluminum fluoride when large amounts of fluoride are added. The composition of this isolated fraction could be $Al_xF_y \cdot nH_2O$.

**$^1$H MAS NMR.** The $^1$H MAS NMR spectra of alumina and fluorinated alumina are shown in Figure 3. The spectrum of the alumina before fluorination exhibits two main peaks at −0.3 and 1.9 ppm, which are assigned to the basic and acidic hydroxyl groups on the surface of alumina, respectively.[16,17] After quantitative decomposition of the spectrum, a broad shoulder at around 5.2 ppm can also be identified. It is ascribed to a small amount of physisorbed and chemisorbed water on the alumina surface.[16,18] Quantitative analysis of the spectrum shows that the number of acidic hydroxyls on the alumina is much larger than that of the basic hydroxyls (Table 2). This indicates that the surface of alumina is mainly acidic. The total amount of surface hydroxyls is 1.43 mmol/g on the fluorine-free alumina, which is quantitatively calculated from the peak areas

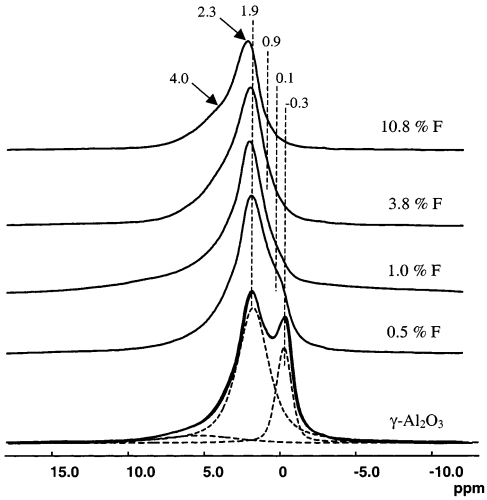


**Figure 3.** $^{1}$H MAS NMR spectra of $\gamma$-$Al_2O_3$ with different fluoride loadings, recorded with a sample spinning rate of 10 kHz and 400 scans. The $^{1}$H MAS NMR spectrum of $\gamma$-$Al_2O_3$ can be decomposed using three Gaussian−Lorentzian lines.

**TABLE 2: Concentrations of Hydroxyls and Fluoride in $Al_2O_3F$ (mmol/g of $Al_2O_3$)**

| F loading (wt %) | amount of acidic hydroxyls | amount of basic hydroxyls | total amount of hydroxyls | reduction of total amount of hydroxyls | addition of fluoride |
|---|---|---|---|---|---|
| 0 | 1.12 | 0.31 | 1.43 | 0 | 0 |
| 0.5 | 1.02 | 0.16 | 1.18 | 0.25 | 0.26 |
| 1.0 | 0.90 | 0.03 | 0.93 | 0.50 | 0.52 |
| 3.8 | 0.49 | 0.02 | 0.51 | 0.92 | 2.08 |
| 10.8 | 0.38 | 0.01 | 0.39 | 1.04 | 6.37 |

simulated using the line shapes in Figure 3. With a surface area of 216 $m^2$/g for the alumina, this corresponds to 4 OH/$nm^2$, in good agreement with the values (3−5 OH/$nm^2$) reported in the literature. [1,17,19,20] Figure 3 shows that, upon fluorination, the signal at −0.3 ppm is reduced preferentially compared to that at 1.9 ppm. Quantitative results (Table 2) show that the total amount of hydroxyls on the 10.8 wt % F/$\gamma$-alumina is also reduced greatly to 0.39 mmol/g and that the amount of basic hydroxyls is decreased more strongly than that of the acidic hydroxyls upon addition of fluoride. These facts suggest that fluoride replaces the acidic and basic alumina hydroxyl groups at the same time, but that the basic hydroxyl groups are substituted preferentially. Moreover, the position of the residual acidic hydroxyls on the alumina surface shifts to lower field at 2.3 ppm upon fluorination to 10.8 wt %. Meanwhile, a broad shoulder appears at about 4.0 ppm, which could be ascribed to the water in $Al_xF_y{\cdot}nH_2O$. The basic hydroxyls shift to around 0.1 ppm in 1.0 wt % F/$\gamma$-alumina. This shift to lower field is due to the inductive through-lattice effect of the electronegative fluoride.[16] It is clear from Table 2 that the reduction of the total amount of surface hydroxyl groups matches the amount of adsorbed fluoride well when its loading is less than or equal to 1.0 wt %, which indicates that one fluoride substitutes for one alumina hydroxyl group at lower fluoride loadings. When the fluoride content is above 3.8 wt %, the loss of the total alumina hydroxyls is less than the amount of fluoride added.

**$^{19}$F MAS NMR.** The $^{19}$F MAS NMR spectra of $Al_2O_3F$ with different fluoride loadings are shown in Figure 4. Three bands are distinguished at about −132 (S3), −145 (S2), and −161 ppm (S1). At 10.8 wt % fluoride loading, the resonance positions of these three peaks shift to −135, −149, and −163 ppm, respectively (Figure 5). Meanwhile, an additional peak appears

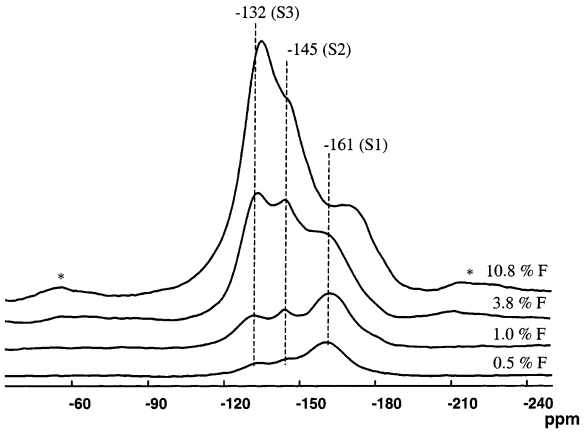


**Figure 4.** $^{19}$F MAS NMR spectra of $\gamma$-$Al_2O_3$ with different fluoride loadings, recorded with ultrafast spinning rate of 29.5 kHz and 1600 scans. Asterisks denote the MAS sidebands.

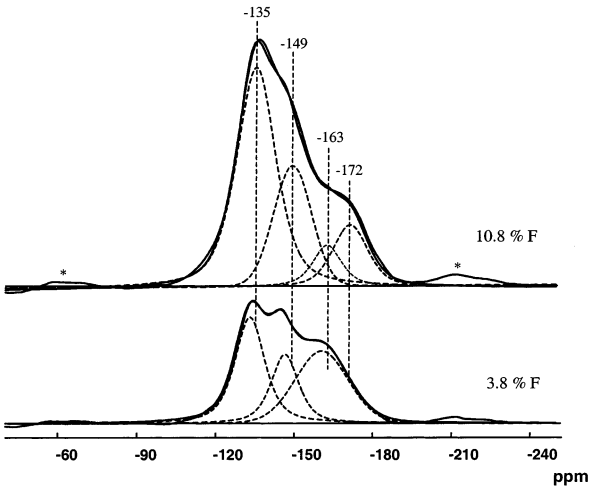


**Figure 5.** $^{19}$F MAS NMR and their simulated spectra of $\gamma$-$Al_2O_3$ with 10.8 and 3.8 wt % fluoride loadings. Asterisks denote the MAS sidebands.

**TABLE 3: Concentrations of Different Fluorine Species in $Al_2O_3F$ (mmol/g of $Al_2O_3$)**

| F loading (%) | S1 | S2 | S3 | fluoride anions in $Al_xF_y{\cdot}nH_2O$ | total |
|---|---|---|---|---|---|
| 0.5 | 0.16 | 0.04 | 0.06 | 0 | 0.26 |
| 1.0 | 0.31 | 0.07 | 0.14 | 0 | 0.52 |
| 3.8 | 0.81 | 0.48 | 0.79 | 0 | 2.08 |
| 10.8 | 0.49 | 1.52 | 3.51 | 0.85 | 6.37 |

at −172 ppm, which could be assigned to $Al_xF_y{\cdot}nH_2O$.[15] This is consistent with the above results from $^{27}$Al MAS and $^{1}$H MAS NMR. Furthermore, Figure 4 also shows that the whole $^{19}$F MAS NMR spectral width is larger with increasing fluoride content. This indicates that residual $^{19}$F−$^{19}$F and $^{19}$F−$^{1}$H dipolar couplings still exist even though an ultrafast magic angle spinning rate (29.5 kHz) was employed in our study. After quantitative decomposition and integration of the spectra, the concentrations of these three types of fluorine species on fluorinated alumina were determined (Table 3). The S1 species are predominant at lower fluoride loadings and decrease at the high fluoride loading of 10.8 wt %. The S3 species increase more readily at higher fluoride loadings. Below the level of around 2.7 wt % fluoride content for the full substitution of 1.43 mmol hydroxyls per gram alumina, the formation of a distinct aluminum fluoride phase is not expected. At 3.8 wt % F, which is above the full hydroxyl substitution, there is no

**SCHEME 1: Proposed Structures for the Six Types of Hydroxyl Groups on the Surface of $\gamma$-$Al_2O_3$ (from refs 1 and 21).**

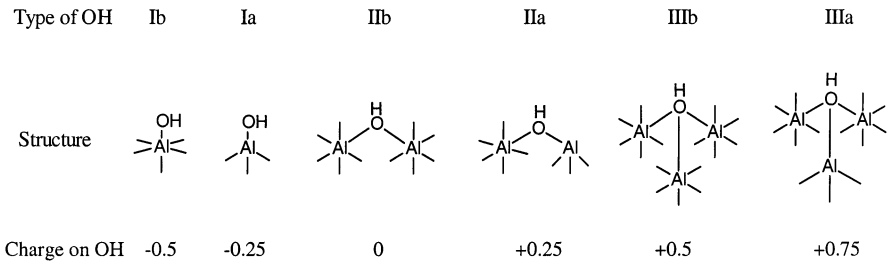


formation of isolated aluminum fluoride either. When the fluoride loading is as high as 10.8 wt %, the content of the fluoride anions in the isolated aluminum fluoride could be 0.85 mmol/g.

## Discussion

Upon fluorination, the concentration of alumina hydroxyl groups recorded by $^1$H MAS NMR decreased. At lower F loadings, quantitative analysis showed that the decrease equals the amount of added fluoride. This indicates that fluorine enters the surface of alumina by substituting hydroxyl groups without breaking the bridging Al−O−Al bonds. At higher F loadings, the decrease in the amount of alumina hydroxyl groups is smaller than the amount of added fluoride, suggesting that bridging Al−O−Al bonds will be broken to adsorb more fluoride and eventually to form isolated $Al_xF_y \cdot nH_2O$ under the strong electron-withdrawing effect of fluorine. This is in agreement with the results of the BET measurements and $^{27}$Al MAS NMR.

The surface hydroxyl groups of alumina can be roughly divided into two groups centered at −0.3 and 1.9 ppm before fluorination. Each group consists of a superposition of several resonances characterizing different hydroxyl structures.[10,16] The signals at lower field represent hydroxyl groups with stronger acidity, whereas the signals at higher field correspond to hydroxyl groups with stronger basicity. Knözinger and Ratnasamy[1] proposed five types of surface hydroxyl groups, Ia, Ib, IIa, IIb, and IIIb (Scheme 1), and Tsyganenko and Mardilovich believed that type IIIa hydroxyl groups probably exist as well.[21] Therefore, six possible types of hydroxyl groups exist on the surface of alumina (Scheme 1). The hydroxyl groups in these various configurations bear slightly different net charges. The higher the negative charge on the hydroxyl group (as in type Ib), the more difficult it will be to remove a proton. Thus, the Brønsted acidity of the hydroxyl groups will decrease, and their basicity will increase as the net charge on the hydroxyl groups becomes more negative.

DeCanio et al. determined the resonances of five types of hydroxyl groups using deuterated $\gamma$-$Al_2O_3$.[16] The signal at −0.3 ppm (Figure 3) for the alumina without fluorine represents the most basic hydroxyl groups of type Ib, whereas the broad signal at 1.9 ppm represents the bridging acidic hydroxyl groups of types II and III.[10,16] Upon fluorination, the ease of removal of hydroxyl groups should parallel their negative charge, because the remaining net positive charge at the vacancy is lower when the exiting hydroxyl group has a higher net negative charge. Therefore, fluoride preferentially displaces hydroxyl groups of type Ib to produce a predominance of S1 fluorine species on the surface of low-F modified alumina, as revealed by the $^{19}$F MAS NMR spectra.

Three peaks were recorded in the $^{19}$F MAS NMR spectrum of $Al_2O_3F$ (Figure 4). Fischer et al. assigned the three resonance

**SCHEME 2: Our Proposed Structures for the Three Types of Fluorine Species on the Surface of Fluorinated $\gamma$-$Al_2O_3$.**

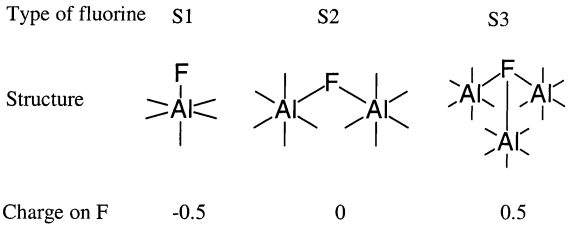


to $Al(O_5F)$, $Al(O_4F_2)$, and $Al(O_3F_3)$ from high field to low field; that is, the aluminum atom is coordinated by one, two, or three fluorine atoms, respectively, in these three structures.[15] From the $^1$H MAS NMR results, we know that the Al−F entities were formed by the replacement of hydroxyl groups by fluoride without breaking the bridging Al−O−Al bonds at lower fluoride loadings. Although it is possible that one aluminum atom binds to two hydroxyl groups at edges of microcrystals and to three hydroxyl groups at the corners,[21] such structures have very high negative charges (−1.0 and −1.5, respectively). It is very unlikely that significant amounts of the corresponding $Al(O_4F_2)$ and $Al(O_3F_3)$ structures exist at lower fluoride loadings. Furthermore, the fact that $Al_xF_y \cdot nH_2O$ has a $^{19}$F resonance at higher field than the S1, S2, and S3 peaks (Figure 5) also contradicts the proposal that the fluorine species corresponding to the low field peak (S3) have an $Al(O_3F_3)$ structure. The assignment of $Al(O_4F_2)$ and $Al(O_3F_3)$, as proposed by Fischer et al., is therefore unlikely.

In contrast to the proposal by Fischer et al., we assign the three types of fluorine entities (Scheme 2), corresponding to the displacement of types I, II, and III hydroxyl groups. From the above $^{27}$Al CP/MAS NMR results, we know that most of the alumina hydroxyl groups are connected to six-coordinated aluminum. Meanwhile, Fischer et al. proved that all fluoride anions on the alumina are coupled to octahedral aluminum.[15] Therefore, we took all of the aluminum atoms in Scheme 2 in octahedral configuration. A fluoride anion that replaces a type Ib hydroxyl group would lead to a S1 type fluorine. Similarly, replacing types IIb and IIIb hydroxyl groups by fluoride anions would give S2 and S3 types of fluorine. Like the hydroxyl groups in structures Ib, IIb, and IIIb (Scheme 1), the S1, S2, and S3 fluorine species bear different charges, being −0.5, 0, and +0.5 for S1, S2, and S3 types of fluorine, respectively. Accordingly, the three peaks in Figure 4 should correspond to S1, S2, and S3 from the high field to the low field. Fluorine bound to one aluminum (S1) is the major species on the low-F modified samples (Table 3). This is consistent with the fact that type Ib hydroxyl groups were preferentially displaced (Figure 3). At higher fluoride loadings, the bridging Al−O−Al bonds in the alumina will be broken to produce more hydroxyl groups

with stronger acidity under the inductive effect of fluorine. At the same time, more acidic hydroxyl groups are replaced by fluoride anions to form the S3 and S2 fluorine species predominating in the $^{19}$F MAS NMR spectra (Figure 4). When the fluoride content is as high as 10.8 wt %, multiple fluoride substitutions on the aluminum atoms in the structures of S1, S2, and S3 will occur, which leads to a shift in their resonance positions to higher field.

## Conclusions

Information about the state of the $\gamma$-alumina surface upon successive impregnation with aqueous solutions of ammonium fluoride was obtained by multinuclear solid-state NMR. At lower fluoride loadings, the basic hydroxyl groups on the alumina surface are replaced preferentially by fluoride compared to the acidic hydroxyl groups. Quantitative $^1$H MAS NMR showed that this kind of substitution occurs stoichiometricly, without breaking the surface Al−O−Al bonds. When the fluoride content is higher than that corresponding to full hydroxyl substitution, more acidic hydroxyl groups are replaced by breaking of surface Al−O−Al bonds, and finally isolated $Al_xF_y{\cdot}nH_2O$ appears under the inductive effect of the electronegative fluorine. $^{19}$F MAS NMR detected three types of fluorine species. Corresponding to the structures of the hydroxyl groups on the surface of alumina, these three types of fluorine species could be assigned to types S1 (fluorine coordinated by one aluminum atom), S2 (fluorine coordinated by two aluminum atoms), and S3 (fluorine coordinated by three aluminum atoms), respectively.

**Acknowledgment.** We thank Dr. Roland Hany of the Federal Laboratories for Materials Testing and Research (EMPA, Dübendorf, Switzerland) for his assistance with the NMR experiments. We also thank the anonymous reviewers for their helpful discussion and suggestions.

**Supporting Information Available:** Fitting parameters for each line in each spectrum of $^1$H and $^{19}$F MAS NMR. This material is available free of charge via the Internet at http://pubs.acs.org.

## References and Notes

(1) Knözinger, H.; Ratnasamy, P. *Catal. Rev.-Sci. Eng.* **1978**, *17*, 31.
(2) Gosh, A. K.; Kydd, R. A. *Catal. Rev.-Sci. Eng.* **1985**, *27*, 539.
(3) Papadopoulou, Ch.; Lycourghiotis, A.; Grange, P.; Delmon, B. *Appl. Catal.* **1988**, *38*, 255.
(4) Benitez, A.; Ramirez, J.; Fierro, J. L. G.; Lopez Agudo, A. *Appl. Catal.* **1996**, *144*, 343.
(5) Boorman, P. M.; Kydd, R. A.; Sarbak, Z.; Somogyvari, A. *J. Catal.* **1987**, *106*, 544.
(6) Benitez, A.; Ramirez, J.; Vazquez, A.; Acosta, D.; Lopez Agudo, A. *Appl. Catal.* **1995**, *133*, 103.
(7) Sun, M.; Prins, R. *J. Catal.* **2001**, *203*, 192.
(8) Okamoto, Y.; Imanaka, T. *J. Phys. Chem.* **1988**, *92*, 7102.
(9) Harris, R. K.; Jackson, P. *Chem. Rev.* **1991**, *91*, 1427.
(10) Kraus, H.; Prins, R. *J. Catal*. **1996**, *164*, 260.
(11) Müller, M.; Harvey, G.; Prins, R. *Micropor. Mesopor. Mater.* **2000**, *34*, 281.
(12) Zhang, W.; Ma, D.; Han, X.; Liu, X.; Bao, X.; Guo, X.; Wang, X. *J. Catal.* **1999**, *188*, 393.
(13) Morris, H. D.; Ellis, P. D. *J. Am. Chem. Soc.* **1989**, *111*, 6045.
(14) Massiot, D.; Fayon, F.; Capron, M.; King, I.; Alonso, S. B.; Durand, J.-O.; Bujoli, B.; Gan, Z.; Hoatson, G. *Magn. Reson. Chem.* **2002**, *40*, 70.
(15) Fischer, L.; Harlé, V.; Kasztelan, S.; d′Espinose de la Caillerie, J. B. *Solid State Nucl. Magn. Reson.* **2000**, *16*, 85.
(16) DeCanio, E. C.; Edwards, J. C.; Bruno, J. W. *J. Catal.* **1994**, *148*, 76.
(17) Jacobsen, C. J. H.; Topsøe, N. Y.; Topsøe, H.; Kellberg, L.; Jakobsen, H. J. *J. Catal.* **1995**, *154*, 65.
(18) Hunger, M.; Freude D.; Pfeifer H. *J. Chem. Soc., Faraday Trans.* **1991**, *87*, 657.
(19) Massoth, F. E. *J. Catal.* **1975**, *36*, 164.
(20) Miciukiewicz, J.; Quader, Q.; Massoth, F. E. *Appl. Catal.* **1989**, *49*, 247.
(21) Tsyganenko, A. A.; Mardilovich, P. P. *J. Chem. Soc., Faraday Trans.* **1996**, *92*, 4843.